

# Modeling the Impact of Silver Particle Size and Morphology on the Covering Power and Tone of Photothermographic Media

Steven H. Kong<sup>†</sup>

Health Group, Eastman Kodak Company, 1 Imation Way, Oakdale, Minnesota 55128

Joel D. Shore

Kodak Research Laboratories, Eastman Kodak Company, 1999 Lake Avenue, Rochester,  
New York 14650-2118

E-mail: joel.shore@kodak.com

---

**Abstract.** *In order to study the effect of the silver particle morphologies in photothermographic images, we calculate exactly the scattering and absorption cross sections for a few distinct morphologies representing simplified limits of the morphologies actually seen in photothermographic images. In particular, we consider isolated spheres, isolated prolate spheroids, and isolated  $3 \times 3 \times 3$  clusters of spheres. These results are then extended to compute approximately the covering power and tone in a slab containing a collection of such scattering and absorbing particles by using the solution to the telegrapher's equation that models the propagation of the light in a medium under the assumption that the light is scattered isotropically by the particles. The anisotropy of the scattering is treated using a widely-used approximate correction that is shown to give reasonably good agreement with a Monte Carlo simulation of the light propagation for the case when the particles are spheres. Our results show that, for solid silver spheres, there is an optimum diameter of approximately 100 nm that yields the highest covering power and the most neutral tone. Higher covering power can be obtained using prolate spheroids having a diameter of 40 nm and a length of about twice that. However, as the aspect ratio of the spheroid increases beyond this, the covering power decreases fairly rapidly, thus suggesting that isolated filaments are not optimal. Finally, the results using clusters of spheres suggest that when the spheres are packed close together the covering power can be greater than that of an isolated sphere containing the same volume of silver as the cluster. © 2007 Society for Imaging Science and Technology. [DOI: 10.2352/J.ImagingSci.Technol.(2007)51:3(235)]*

---

## INTRODUCTION

Images from conventional black-and-white photography are generated by small silver particles, which are typically in the form of filaments.<sup>1</sup> Photothermographic images generated from silver carboxylates can be filamentary or round. The filamentary particle is a solid strand of silver. The round particle is typically an agglomeration of spherical 5–30 nm diameter nanoparticles of silver and has been called a dendrite in the literature.<sup>2</sup> The size and morphology of the silver have an impact on the absorption and scattering spectrum

and thus impact the tone and covering power of the image. It would be very useful to have the capability to calculate the covering power and tone given the concentration, size, and morphology of the silver particles. However, to perform such a calculation on the complex Ag particle morphologies seen in the film is not a trivial matter, so simplifications necessarily must be made.

The simplest approximation for covering power (the image optical density achieved per unit coverage of silver) is based on the Nutting model, which uses the projection area of the silver particles.<sup>3,4</sup> However, this does not give correct results because the actual extinction cross section for small particles is not equal to the geometric cross section. In order to correct for this, Farnell and Solman introduce a correction factor.<sup>5</sup> In order to quantify this correction factor, the absorption cross section of the silver particles needs to be calculated. The absorption cross sections of isolated silver spheres and prolate spheroids can be calculated directly from Mie theory<sup>6</sup> and T-matrix formalism,<sup>7</sup> respectively. The calculation for a cluster of noncontacting silver spheres is much more difficult, especially for cluster sizes that are typically observed for photothermographic materials.<sup>2</sup> Recently, code from Mackowski et al. has been used to calculate the extinction and scattering cross sections for infinite silver cylinders, linear chains of up to three silver spheres, and a small cubic cluster that consists of eight silver spheres.<sup>8</sup> These results show the importance of the distance between the silver nanoparticles in the cluster.

With the extinction cross section of the silver particles that make up an image, the covering power can be calculated using the Nutting model for the geometry of specular transmission. The Nutting model does not address the diffuse transmission of light. However, in practical situations, the total transmission is much more relevant. Obtaining the total transmission for a random distribution of particles given the extinction and scattering cross sections for these individual particles is not a trivial task. Assuming the particles are far enough apart to be treated independently, one can use a geometric optics approach to follow the path of the

---

<sup>†</sup>Present address: 3M Corporation, 3M Center, Building 235-2S-62, St. Paul, Minnesota 55144-1000. E-mail: shkong@mmm.com

Received Sep. 11, 2006; accepted for publication Oct. 6, 2006.

1062-3701/2007/51(3)/235/8/\$20.00.

light between the scattering or absorption events. In this case, an accurate solution can be obtained using Monte Carlo Simulation.<sup>9</sup> However, this approach is time-consuming and more practical approaches have typically been used. The most widely used approximation is the Kubelka-Munk theory.<sup>10</sup> However, this is not very applicable to media with high absorption. More recently, the topic of photon transmission in turbid media has generated great interest in both soft, condensed matter physics and medical diagnostics.<sup>11</sup> In this paper, we adopt the approach based on the telegrapher's equation.<sup>11</sup> Details of this approach and the general topic of photon transmission in a turbid slab will be addressed more extensively elsewhere.<sup>12</sup> Here, we extend the work in Ref. 8 to include larger clusters of silver spheres and finite-sized filaments modeled as spheroids and use these results and the solution obtained from the telegrapher's equation to perform calculations for covering power and tone.

### CROSS SECTIONS

The calculations for extinction, scattering, and absorption cross sections are carried out in a manner similar to Ref. 8 for an isolated silver sphere, an isolated silver spheroid, and a cluster of silver spheres immersed in a medium of refractive index  $n=1.481$ . The spectrally dependent refractive index for Ag is taken from Hagemann<sup>13</sup> interpolated over the spectrum; in all cases except the spheroid, corrections are made to the refractive index for particle size as discussed in Ref. 8. (Such size corrections generally have a small effect, and whether or not they are performed does not affect any of the conclusions here.) The calculations are based on exact solutions of the problem defined by plane-wave electromagnetic radiation incident on the isolated object; however, because they involve expansions with an infinite number of terms, the expansions must be truncated once the numerical errors are small enough. Mie theory is used for the isolated silver spheres, a T-matrix code is used for the spheroids,<sup>7</sup> and codes from Xu<sup>14</sup> and from Mackowski et al.<sup>15</sup> are used for the clusters of silver spheres. The code from Xu is based on computing the interaction terms between the spheres and thus converges most rapidly for large separation distances when these interactions are small. By contrast, the code from Mackowski et al. is based on considering the cluster as a single object from which the scattering is then calculated using a multipole field expansion. It thus requires fewer terms in the expansion when the cluster is more compact, i.e., when the separation distances are small. Both codes give the same results except at very small separation distances where Xu's code does not converge as well. Therefore, the Mackowski et al. code is used in the short- to mid-range separation distances, and the Xu code is used in the mid- to long-range separation distances. (When the spheres are practically touching, neither code converges well. Hence, we have set the shortest distance that we consider such that the results from the Mackowski et al. code is insensitive to significant changes in the convergence criteria.)

The Mie theory results for isolated silver spheres are

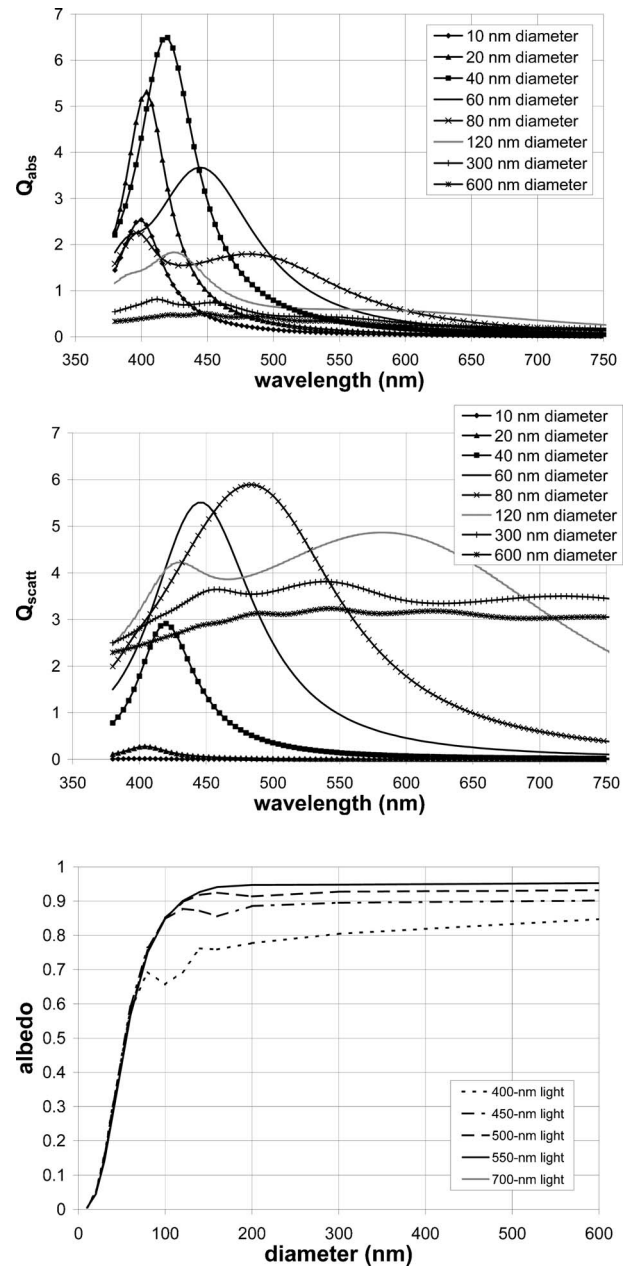


Figure 1. Calculated  $Q_{abs}$  (top) and  $Q_{scatt}$  (middle) spectra for isolated silver spheres of various diameters. The albedo ( $Q_{scatt}/Q_{ext}$ ) versus diameter for several wavelengths of light (bottom).

shown in Figure 1. We consider the scattering, absorption, and extinction efficiencies ( $Q_{scatt}$ ,  $Q_{abs}$ ,  $Q_{ext}$ ), which are defined as the corresponding cross sections divided by the geometric cross section  $\pi r^2$  where  $r$  is the radius of the sphere; note that  $Q_{ext} = Q_{scatt} + Q_{abs}$ . The spectra for the cross sections and the albedo ( $Q_{scatt}/Q_{ext}$ ) are a strong function of the silver sphere diameter. At small diameters, the spectra for the cross sections peak in the near UV region of the spectra, which is not ideal for blocking visible light. At larger diameters, the peak shifts into the blue and then the spectrum flattens out, but  $Q_{abs}$  becomes quite low and the albedo becomes very high, which gives poor covering power. Later it will be shown that there is an ideal diameter for maximizing the covering power.

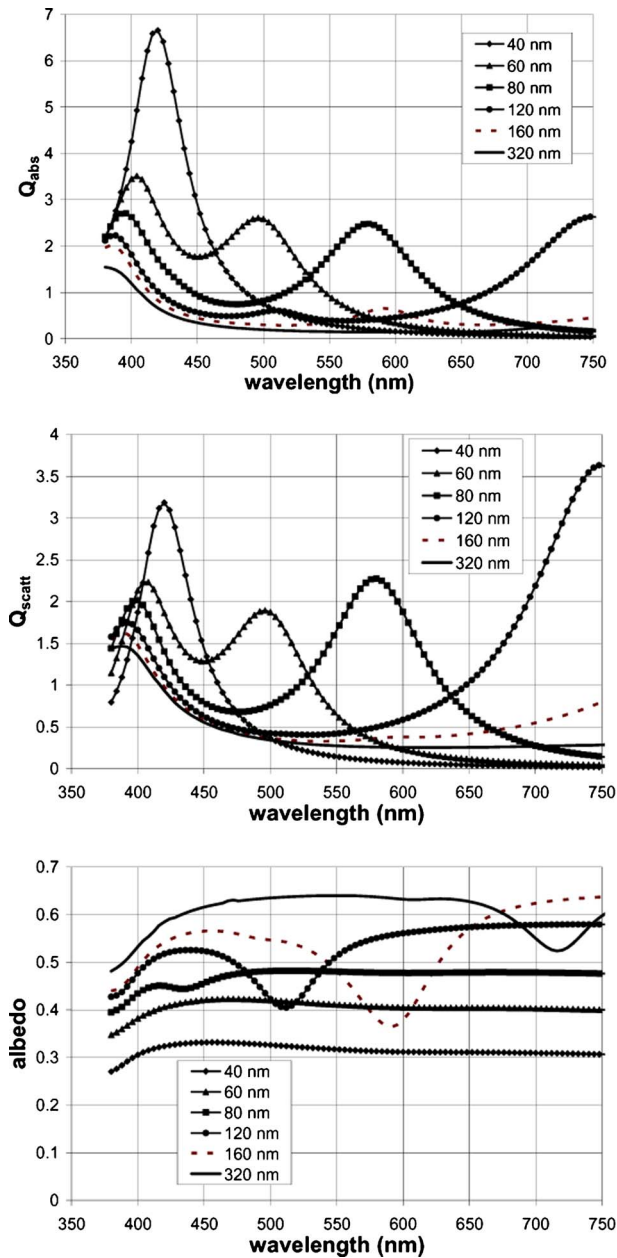


Figure 2. Calculated  $Q_{abs}$  (top),  $Q_{scatt}$  (middle), and albedo (bottom) spectra for isolated randomly oriented 40 nm diameter prolate silver spheroids with the various lengths given in the legend.

The results for isolated randomly oriented prolate (“cigar-shaped”) silver spheroids are shown in Figure 2. Here,  $Q_{scatt}$ ,  $Q_{abs}$ , and  $Q_{ext}$  are the scattering, absorption, and extinction cross sections divided by  $\pi ab$ , where  $a$  and  $b$  are the lengths of the semi-axes. The spectra for the cross sections and the albedo ( $Q_{scatt}/Q_{ext}$ ) are a strong function of the spheroid length. In particular, the peak in the far blue

end of the spectrum for a perfect sphere splits into two peaks as the aspect ratio of the spheroid increases. One peak shifts slowly to lower wavelengths as the other shifts more rapidly to higher wavelengths. There appears to be an optimal length where the absorption cross section peaks in the visible spectrum. If the spheroid is too long, the absorption cross section peaks in the ultraviolet and the near infrared spectra. In addition, the albedo increases with increasing length. The implications on the covering power of filaments will be explored in the following section.

The results for a randomly oriented  $3 \times 3 \times 3$  cubic array of twenty-seven 10 nm diameter silver spheres at various separation distances are shown in Figure 3. The results for a  $3 \times 3 \times 3$  cubic array of 20 nm diameter silver spheres are shown in Figure 4. Here,  $Q_{scatt}$ ,  $Q_{abs}$ , and  $Q_{ext}$  are the scattering, absorption, and extinction cross sections divided by the geometric cross section of an equivalent-volume sphere. The separation distance is the distance between surfaces for the nearest-neighbor spheres in a cluster. The silver clusters absorb at longer wavelengths and with less scattering than does a solid sphere of equivalent volume. Calculations for a dendrite of a more realistic size, such as a cluster of several hundred 10 nm diameter spheres, would require very extensive computing power, which is beyond the scope of this study.

### Covering Power

#### Method for Calculating Covering Power

Of particular interest for a silver image is its covering power, which is the image density achieved per unit coverage of silver. In a photothermographic media based on silver carboxylate, the latent image catalyzes the chemical reduction of silver carboxylate to neutral silver atoms ( $Ag^0$ ). The covering power (CP) will be defined as follows:

$$CP = (D - D_0)/Ag^0Wt, \tag{1}$$

where  $Ag^0 Wt$  is the amount of  $Ag^0$  per unit area of the imaged film.  $D - D_0$  is the image density contribution by the  $Ag^0$  particles.  $D$  is the image density of the processed film.  $D_0$  is the contribution to the density by components other than  $Ag^0$  such as the base, silver halide, silver carboxylates, and dyes. This can be taken as the unprocessed density assuming there are no heat-bleachable dyes or thermally generated dyes, or it can be understood as the processed  $D_{min}$  assuming there is negligible contribution from fog centers.

The covering power is obtained by using the calculated spectra for the absorption and scattering cross sections as input to the following relationship for total transmission:<sup>12</sup>

$$T = \frac{\eta qs \exp[-\epsilon d]((\epsilon s + \eta q^2)(\exp[\epsilon d] - \cosh[qd]) - q(\eta \epsilon + a)\sinh[qd])}{(\epsilon^2 - q^2)(2\eta qd \cosh[qd] + (\eta^2 q^2 + a^2)\sinh[qd])} + \exp[-\epsilon d], \tag{2}$$

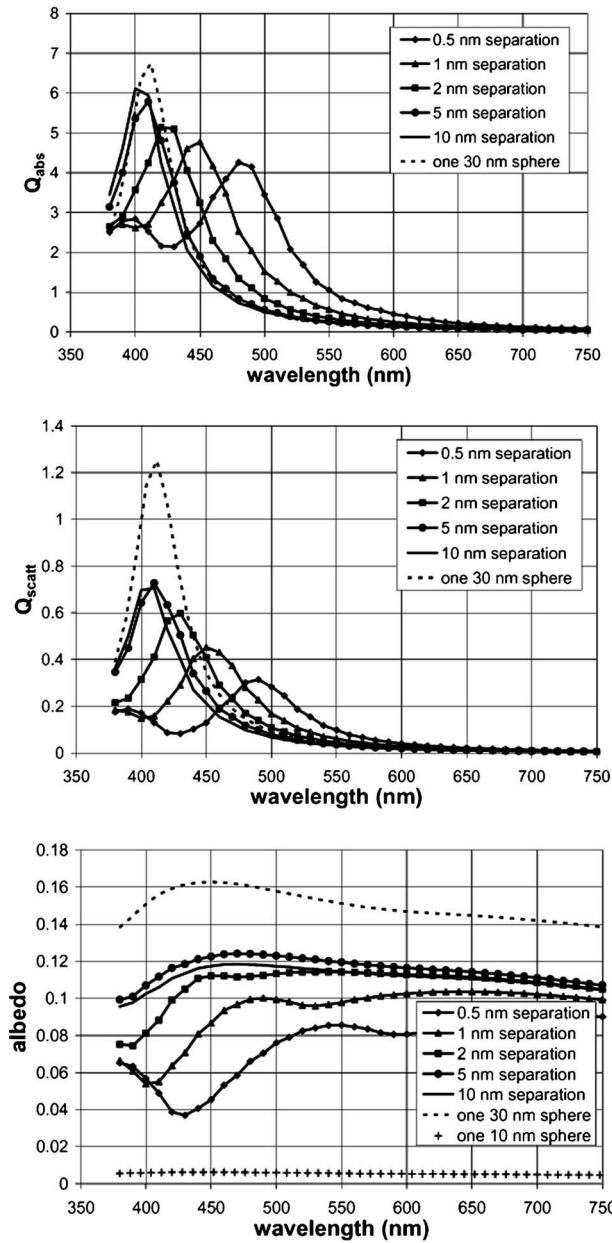


Figure 3. (Solid lines) Calculated  $Q_{\text{abs}}$  (top),  $Q_{\text{scatt}}$  (middle), and albedo (bottom) spectra for randomly oriented  $3 \times 3 \times 3$  cubic arrays of twenty-seven 10 nm diameter silver spheres at various separation distances (as specified by the distance of closest approach between the surfaces of neighboring spheres).  $Q_{\text{abs}}$  and  $Q_{\text{scatt}}$  are the calculated absorption and scattering cross sections normalized by the geometric cross section of a single sphere of equivalent volume, i.e., 30 nm in diameter. Data for a single 30 nm diameter sphere (dotted line) and (in the case of the albedo) for a single 10 nm diameter sphere (crosses) are included for comparison.

where

$$a = \sigma_A n, \tag{3}$$

$$s = \sigma_S n, \tag{4}$$

$$\varepsilon = a + s, \tag{5}$$

$$q^2 = 3a(a + \beta s), \tag{6}$$

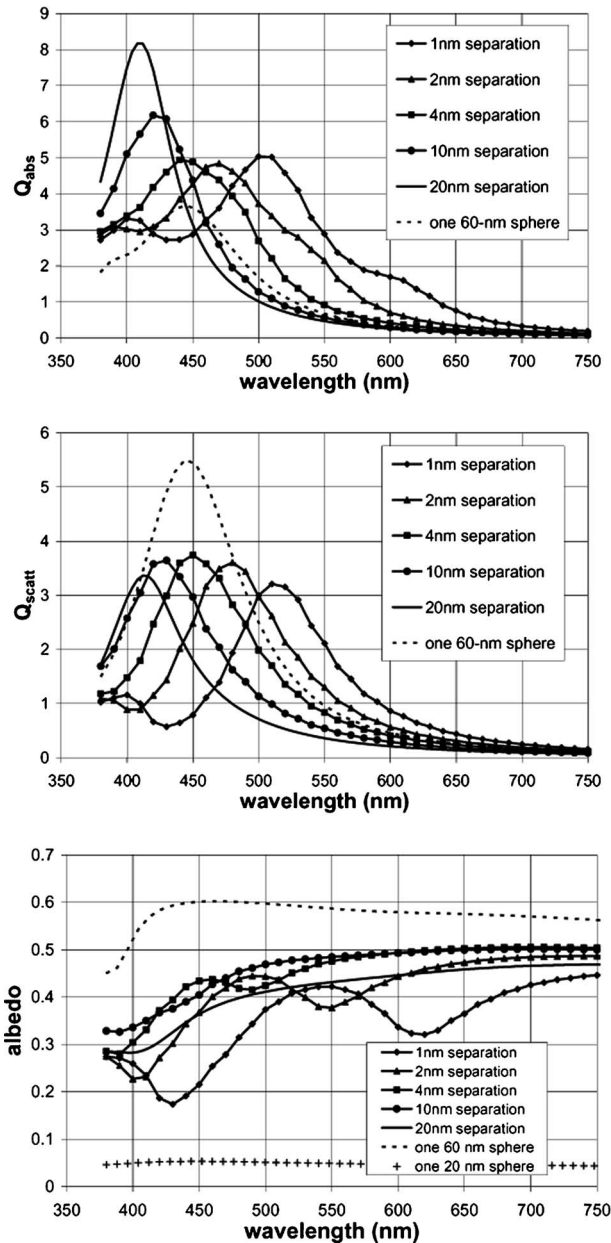


Figure 4. (Solid lines) Calculated  $Q_{\text{abs}}$  (top),  $Q_{\text{scatt}}$  (middle), and albedo (bottom) spectra for randomly oriented  $3 \times 3 \times 3$  cubic arrays of twenty-seven 20 nm diameter silver spheres at various separation distances.  $Q_{\text{abs}}$  and  $Q_{\text{scatt}}$  are the calculated absorption and scattering cross sections normalized by the geometric cross section of a single sphere of equivalent volume, i.e., 60 nm in diameter. Data for a single 60 nm sphere (dotted line) and (in the case of the albedo) for a single 20 nm sphere (crosses) are included for comparison.

$$\eta c = -j(0)/p(0) = j(d)/p(d). \tag{7}$$

$a$ ,  $s$ , and  $\varepsilon$  are the absorption, scattering, and extinction coefficients.  $\sigma_A$  and  $\sigma_S$  are the absorption and scattering cross sections,  $d$  is the layer thickness,  $n$  is the number of silver particles per unit volume, and  $c$  is the speed of light.  $j(z)$  is the photon “current density” at  $z$  and  $p(z)$  is the photon concentration at  $z$ . For the calculations in this paper,  $\eta$  and the constant  $\beta$  are set to  $1/2$ .

Equation (2) was derived using the telegrapher’s differential equation to model the photon diffusion in a turbid

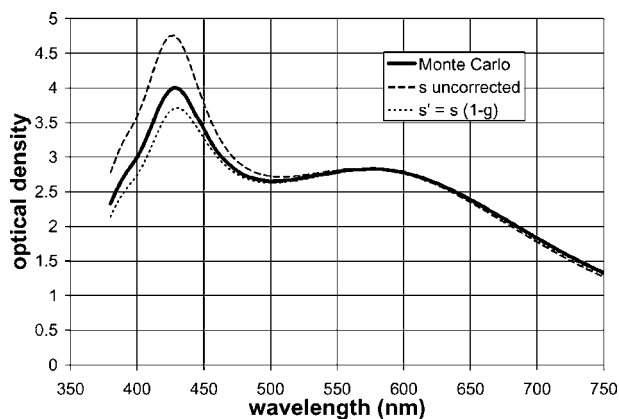


Figure 5. The optical density for total transmission through a slab with a dispersion of 120 nm diameter silver spheres calculated using Eq. (2) with and without correction for anisotropy. These results are compared to the exact solution of the radiative transfer problem obtained by Monte Carlo.

media.<sup>11</sup> Reflections at the interfaces were ignored in this calculation, and the scattering was assumed to be isotropic. Details of the calculation can be found in Ref. 12. The resulting total transmission spectrum was used to calculate a visual density, which is taken to be  $-\log_{10}(Y/Y_n)$ , where  $Y$  is the CIE  $Y$  tristimulus value for the transmitted light, and  $Y_n$  is the CIE  $Y$  tristimulus value for the incident beam.<sup>16</sup> The D65 illuminant was used for these calculations.

#### Incorporating Anisotropy

Equation (2) is calculated for the case of isotropic scattering. Because the scattering of light by small silver particles is in general not isotropic, a correction for anisotropy is needed. The impact of anisotropic scattering can be approximately incorporated by replacing  $s$  with  $s'$  as follows:

$$s' = s(1 - g), \quad (8)$$

where  $g \equiv \langle \cos \theta \rangle$  and  $\theta$  is the scattering angle.<sup>11,17</sup>

The effectiveness of this correction is shown in Figure 5, where the absorption spectrum for a single 120 nm diameter silver sphere calculated using Eq. (2) is corrected for the anisotropy in light scattering using Eq. (8) and compared with the solution obtained using the Monte Carlo method,<sup>9</sup> which incorporates the exact angular dependence for the scattering as derived by Mie theory. (In our implementation of the Monte Carlo method, any polarization of light that can occur because of the scattering and could have an effect on subsequent scattering events is ignored.)

We have recently done more detailed studies<sup>12</sup> comparing Monte Carlo simulations run at different values of anisotropy with the anisotropy implemented using the Henyey-Greenstein scattering function.<sup>18</sup> By doing this, we are able to focus more directly on the accuracy of the anisotropy correction given by Eq. (8) than we can when we compare Monte Carlo simulations to the telegrapher's equation approach because the error in the anisotropy correction described by Eq. (8) is no longer convolved with the error in the use of the telegrapher's equation for  $g=0$ . The reader is referred to this work for more details on the accuracy of this

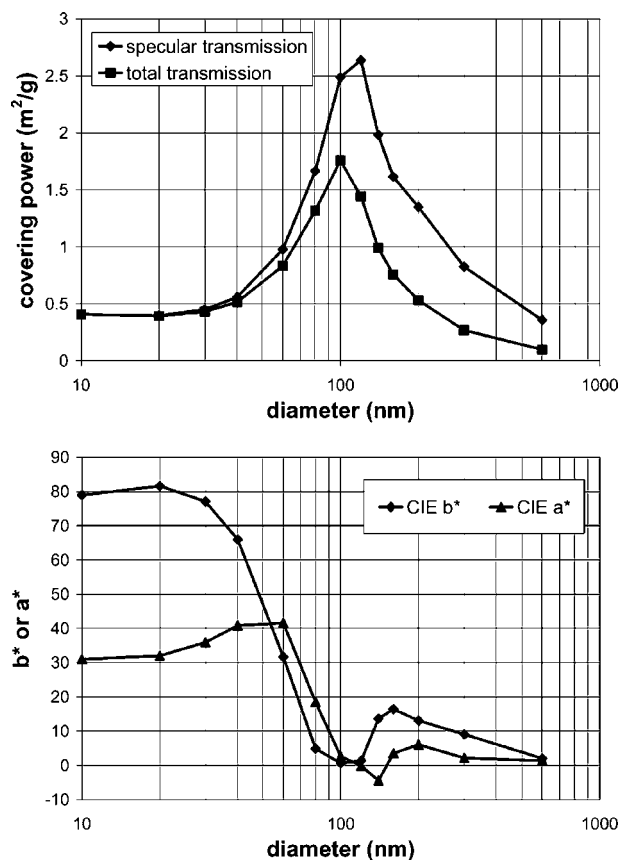


Figure 6. Calculated covering power (top) and CIE  $b^*$  and  $a^*$  (bottom) for solid silver spheres dispersed randomly in a 20  $\mu\text{m}$  layer with a silver loading of 1.9  $\text{g}/\text{m}^2$ . The calculated  $b^*$  and  $a^*$  are for total transmission only.

anisotropy correction. At any rate, for the generally rather modest values of  $g$  that occur for the particle sizes and shapes studied here, this anisotropy correction is expected to be quite adequate.

#### RESULTS

Figure 6 shows the calculated covering power and tone for a 20  $\mu\text{m}$  thick layer containing randomly dispersed silver spheres as a function of the sphere diameter at a constant total Ag loading of 1.9  $\text{g}/\text{m}^2$ . The covering power in the case of specular transmission is calculated by using the extinction cross section in the Nutting formula. The covering power in the case of total transmission is calculated by using Eqs. (1)–(8). The cross sections for the spheres are calculated using Mie theory with size correction in the Ag refractive index values of Hagemann et al.<sup>8,13</sup> and a refractive index of  $n=1.481$  is assumed for the medium. Reflections at any interfaces between the medium and air are ignored. Figure 6 shows that the optimal diameter for a silver sphere is between 100 and 120 nm.

The typical covering power for photothermographic media is between 2 and 3  $\text{m}^2/\text{g}$ .<sup>19</sup> Because the covering power reached for total transmission in Fig. 6 is not this high for any diameter, these results suggest that solid silver spheres are not the optimal morphology for covering power. However, solid silver spheroids with an aspect ratio of about

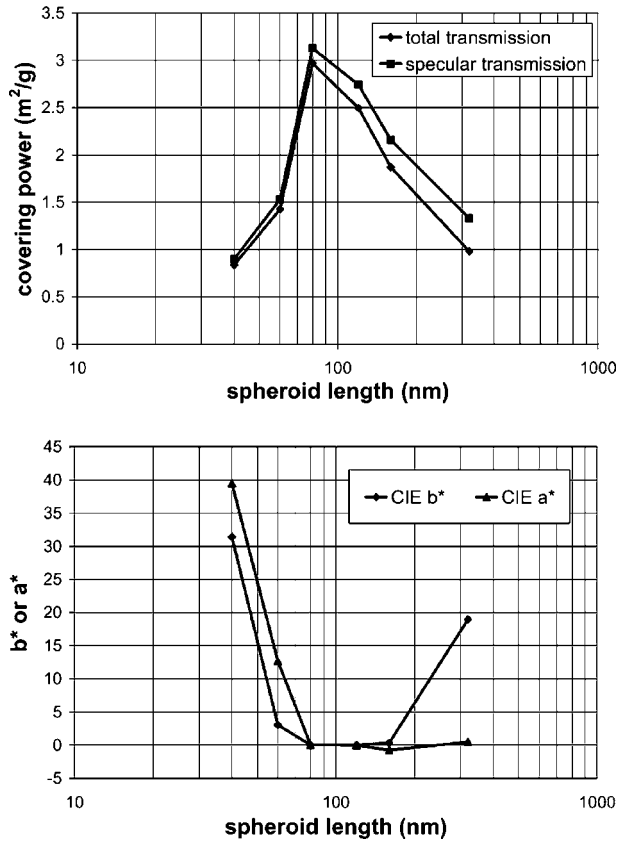


Figure 7. Calculated covering power (top) and CIE  $b^*$  and  $a^*$  (bottom) for 40 nm diameter randomly oriented prolate solid silver spheroids of various lengths dispersed randomly in a  $20 \mu\text{m}$  layer with a silver loading of  $1.9 \text{ g/m}^2$ . The calculated  $b^*$  and  $a^*$  are for total transmission only.

two have a much higher calculated covering power than silver spheres, as can be seen in Figure 7. The calculated covering power deteriorates as the aspect ratio increases, suggesting that long filaments have poor covering power. The tone in both cases is good near the optimal region for covering power but rapidly deteriorates at lower and higher diameters for spheres or lower and higher aspect ratios for spheroids.

The covering power and tone for the cubic array of twenty-seven 10 nm diameter silver spheres and the cubic array of twenty-seven 20 nm diameter silver spheres are calculated for several separation distances in Figure 8 and Figure 9. In these cases (especially for the 10 nm diameter spheres), there is minimal diffuse transmission. The covering power increases as the distance between the spheres in the array decreases. The covering power increases dramatically as the separation distance decreases below the radius of the spheres. In this regime, the covering power is greater than that for the spheres of equivalent volume (a 30 nm diameter sphere in Fig. 8 and a 60 nm diameter sphere in Fig. 9). The results suggest that a cluster of small spheres with sufficiently small separation distance has a more advantageous morphology than does an isolated larger solid sphere. Ideally, larger clusters where light scattering plays a larger role should be studied to verify this conclusion.

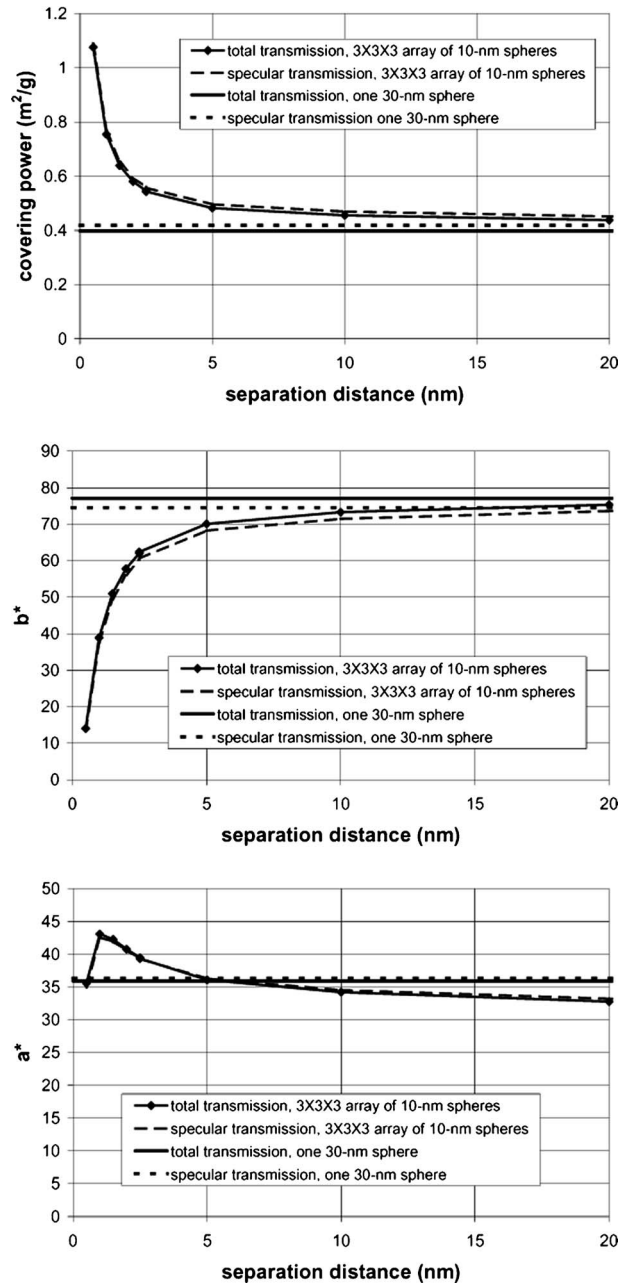


Figure 8. Calculated covering power (top), CIE  $b^*$  (middle) and  $a^*$  (bottom) for randomly oriented  $3 \times 3 \times 3$  cubic clusters of twenty-seven 10 nm diameter silver spheres in a  $20 \mu\text{m}$  layer with a silver loading of  $1.9 \text{ g/m}^2$ . Results for the cluster are compared with the results for a dispersion of isolated silver spheres with equivalent volume.

## DISCUSSION

The results show that the covering power and tone for a dispersion of solid silver spheres has a strong dependence on the diameter. The optimal calculated covering power at about  $0.1 \mu\text{m}$  diameter is less than  $2 \text{ m}^2/\text{g}$ , thus suggesting that solid silver spheres are not ideal. From the calculations for spheroids, it appears that 40 nm diameter spheroids with an aspect ratio of about 2 can give a reasonably high covering power. However, as the aspect ratio increases and the spheroid takes on the shape of a long filament, the covering power decreases and becomes poor. Therefore, this suggests that isolated filaments should have poor covering power.

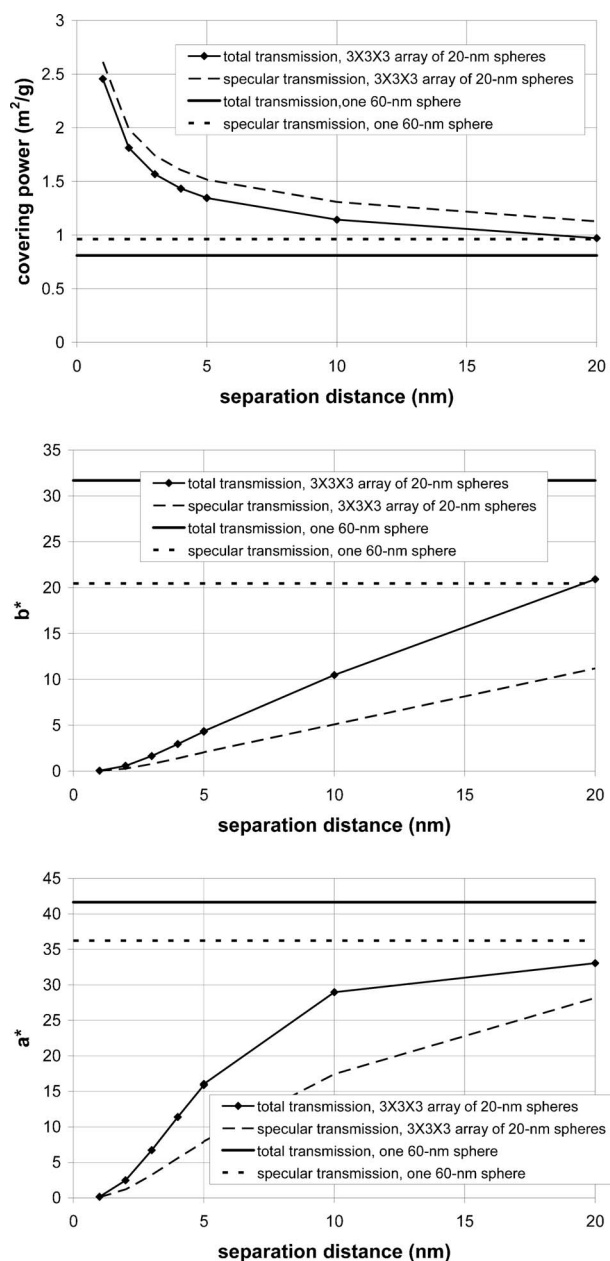


Figure 9. Calculated covering power (top), CIE  $b^*$  (middle) and  $a^*$  (bottom) for randomly oriented  $3 \times 3 \times 3$  cubic clusters of twenty-seven 20 nm diameter silver spheres in a  $20 \mu\text{m}$  layer with a silver loading of  $1.9 \text{ g/m}^2$ . Results for the cluster are compared with the results for a dispersion of isolated silver spheres with equivalent volume.

Because of limitations in computational power, the calculation of covering power for a cluster with a number of silver particles approaching the number observed in TEM micrographs<sup>8</sup> was not feasible. Therefore, the covering power for an ideal cluster of silver particles was not calculated. Another complication is whether the small silver spheres are in electrical contact with each other in an actual dendritic silver particle. If they were in electrical contact, then these calculations might not properly predict the correct covering power given that the code used cannot handle such a scenario. Nevertheless, the results for an array of 27 silver spheres show that noncontacting clusters of small silver spheres can give higher covering power than isolated silver

spheres. This supports the conventional wisdom that clusters of silver spheres are desirable.<sup>8</sup>

The calculations for CIE  $a^*$  and CIE  $b^*$  show that the tone can vary widely. Because a neutral or slightly blue tone is the most desirable, the results show that in most cases, the tone is undesirable. In particular, very small silver spheres (e.g., Carey Lea silver) should give intense colors as has been observed experimentally.<sup>8</sup> Long spheroids should contribute to a light yellow tone. While clusters of small silver spheres can give better tone, this is not the case for the  $3 \times 3 \times 3$  cubic array of 10 nm diameter silver spheres. In this case the covering power is also not very high. In the regions where the covering power is high for the array of 20 nm diameter spheres, the tone is fairly neutral. Furthermore, it must be kept in mind that the visual density is high in these regions so that any color would tend to be suppressed. A more thorough study of tone would involve varying the silver particle concentration to give several different gray levels. This is beyond the scope of this paper.

## SUMMARY

We have calculated the covering power and tone for solid spheres, solid spheroids, and cubic arrays of twenty-seven 10 nm and 20 nm silver spheres. The calculations were performed using theoretical cross sections and a relationship for total transmission derived from the telegrapher's equation. The absorption and scattering coefficients were derived from the absorption and scattering cross sections that were calculated using Mie theory, a T-matrix code from Mishchenko,<sup>7</sup> and codes for clusters of spheres from Mackowski et al.<sup>15</sup> and from Xu.<sup>14</sup> The anisotropy in the scattering by the isolated particles was taken into account using a simple correction factor for the scattering coefficient that has been widely used in the literature.<sup>11,17</sup> The total transmission was estimated using the solution from the telegrapher's equation for a silver loading of  $1.9 \text{ g/m}^2$ . The CIE tristimulus values were calculated from the transmission spectra, which were used to derive the visual density and tone. The results suggest that a cluster of small silver spheres can result in a higher covering power than a single silver sphere of optimal size. In addition, the results for spheroids suggest that stubby filaments may give reasonably good covering power, but long filamentary silver particles would have poor covering power. Therefore, these results give some indication of why the dendritic silver particles in photothermographic materials are ideal and long filaments are not.

## REFERENCES

- W. West and P. B. Gilman, in *The Theory of the Photographic Process*, 4th ed., edited by T. H. James (Macmillan, New York, 1977), p. 255.
- B. B. Bokhonov, L. P. Burleva, D. R. Whitcomb, and M. R. V. Sahyun, *Microsc. Res. Tech.* **42**, 152 (1998).
- P. G. Nutting, *Philos. Mag.* **26**, 423 (1913).
- J. C. Dainty and R. Shaw, *Image Science* (Academic Press, New York, 1974), p. 41.
- G. C. Farnell and L. R. Solman, *J. Photogr. Sci.* **11**, 348 (1963).
- G. Mie, *Ann. Phys.* **25**, 377 (1908).
- M. I. Mishchenko and L. D. Travis, *J. Quant. Spectrosc. Radiat. Transf.* **60**, 309 (1998); Codes "tmd.new.f" and "tmq.new.f" written by M. I. Mishchenko ([http://www.giss.nasa.gov/~crmim/t\\_matrix.html](http://www.giss.nasa.gov/~crmim/t_matrix.html)).
- D. R. Whitcomb, S. Chen, J. D. Shore, P. J. Cowdery-Corvan, and K. A.

- Dunn, J. *Imaging Sci. Technol.* **49**, 370 (2005).
- <sup>9</sup>J. J. DePalma and J. Gasper, *Photograph. Sci. Eng.* **16**, 181 (1972).
- <sup>10</sup>H. G. Völz, in *Industrial Color Testing* (VCH, Weinheim, DE, 1995), p. 93.
- <sup>11</sup>D. J. Durian, *Opt. Lett.* **23**, 1502 (1998).
- <sup>12</sup>S. H. Kong and J. D. Shore, "Beyond the Nutting Formula: Evaluation of methods for calculating optical density from absorption and scattering cross sections", *Proc ICIS '06: The 30th International Congress of Imaging Science* (IS&T, Springfield, VA, 2006) p. 233; S. H. Kong and J. D. Shore, "Evaluation of the telegrapher's equation and multiple-flux theories for calculating the transmittance and reflectance of a diffuse absorbing slab", *J. Opt. Soc. Am. A* **24**, 702 (2007).
- <sup>13</sup>H.-J. Hagemann, W. Gudat, and C. Kunz, *Optical Constants From the Far Infrared to the X-Ray Region: Mg, Al, Cu, Ag, Bi, C, and Al<sub>2</sub>O<sub>3</sub>*, DESY SR-74/7 (Hamburg, DE, 1974); *CRC Handbook of Chemistry and Physics*, edited by D. R. Lide (CRC Press, Boca Raton, FL, 2003).
- <sup>14</sup>Y. Xu, *Phys. Rev. E* **67**, 046620-1 (2003); Code "gmm01TrA.f" written by Y. Xu (<http://www.astro.ufl.edu/~xu>).
- <sup>15</sup>D. W. Mackowski, *J. Opt. Soc. Am. A* **11**, 2851 (1994); Code "scsmtml.for" written by D. W. Mackowski, K. Fuller, and M. I. Mishchenko ([http://www.giss.nasa.gov/~crmim/t\\_matrix.html](http://www.giss.nasa.gov/~crmim/t_matrix.html)).
- <sup>16</sup>CIE Technical Report on Colourimetry CIE 15:2004, 3rd ed.
- <sup>17</sup>A. H. Gandjbakhche, R. F. Bonner, and R. Nossal, *J. Stat. Phys.* **69**, 35 (1992); A. H. Gandjbakhche, R. F. Bonner, and R. Nossal, *Appl. Opt.* **32**, 504 (1993); A. H. Gandjbakhche, R. F. Bonner, and R. Nossal, *Phys. Rev. E* **48**, 810 (1993); Z. Guo and S. Kumar, *Appl. Opt.* **39**, 4411 (2000).
- <sup>18</sup>L. G. Henyey and J. L. Greenstein, *Astrophys. J.* **93**, 70 (1941).
- <sup>19</sup>T. Ohzeki, *IS&T/SPSTJ 2004 International Symposium on Silver Halide Technology* (IS&T, Springfield, VA, 2004) p. 7.